

# STRANGE PARTICLES AND NEUTRON STARS - EXPERIMENTS AT GSI

P. Senger

Gesellschaft für Schwerionenforschung, Planckstr. 1,  
64291 Darmstadt, Germany

Abstract

Experiments on strangeness production in nucleus-nucleus collisions at SIS energies address fundamental aspects of modern nuclear physics: the determination of the nuclear equation-of-state at high baryon densities and the properties of hadrons in dense nuclear matter. Experimental data and theoretical results will be reviewed. Future experiments at the FAIR accelerator aim at the exploration of the QCD phase diagram at highest baryon densities.

PACS numbers: PACS 25.75.Dw

arXiv:nucl-ex/0611010v1 9 Nov 2006

## I. INTRODUCTION

The goal of the nucleus-nucleus collision research program at the present and the future GSI accelerators is to investigate the properties of highly compressed nuclear matter. Such a form of matter exists in various so far unexplored phases in the interior of neutron stars and in the core of type II supernova explosions. Figure 1 illustrates structures of neutron stars as predicted by various models (compilation by F. Weber [1]). As to date, none of these proposed novel phases of subatomic matter can be ruled out by observation. Further understanding of the structure on neutron stars requires more experimental information on the nuclear equation-of-state at high baryon densities, on the in-medium properties of hadrons, in particular of strange particles, and on location of the deconfinement phase transition at high baryon densities.

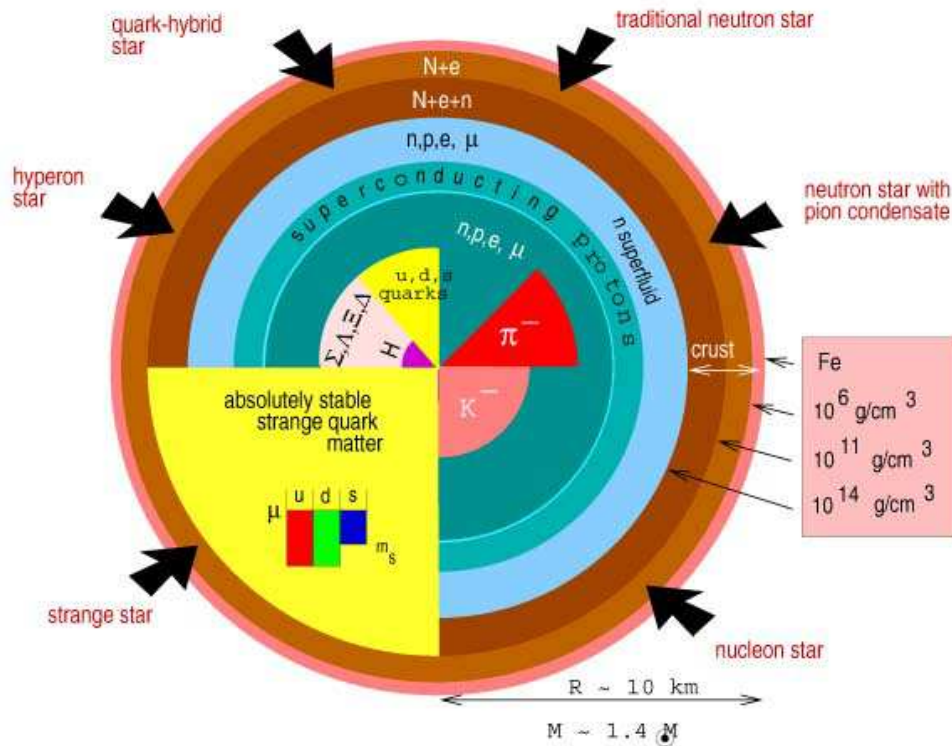


FIG. 1: Structures of neutron stars and novel phases of subatomic matter as predicted by different models (taken from [1])

### A. The nuclear matter equation-of-state

The nuclear matter equation of state plays an important role for the dynamics of core collapse supernova and for the stability of neutron stars. In type II supernova explosions, symmetric nuclear matter is compressed to 2-3 times saturation density. These conditions are realized in heavy-ion collisions at SIS18 beam energies, although the temperatures reached in nuclear collisions are higher than those in the core of a supernova. The isospin asymmetric matter in the interior of neutron stars is compressed to 5 - 10 times saturation density. At these high densities, the nucleons are expected to melt into quarks and gluons. The experimental study of this extreme state of matter in the laboratory will be one of the major research programs at the future Facility for Antiproton and Ion Research (FAIR).

Figure 2 depicts different versions of the equation of state as predicted by different calculations (see [2]). The figure illustrates that it is not sufficient to determine the nuclear compressibility (which is determined by the curvature of  $E(\rho)$  at saturation density), but rather one has to study the response of nuclear matter at different densities, which means one has to perform nucleus-nucleus collisions at different beam energies.

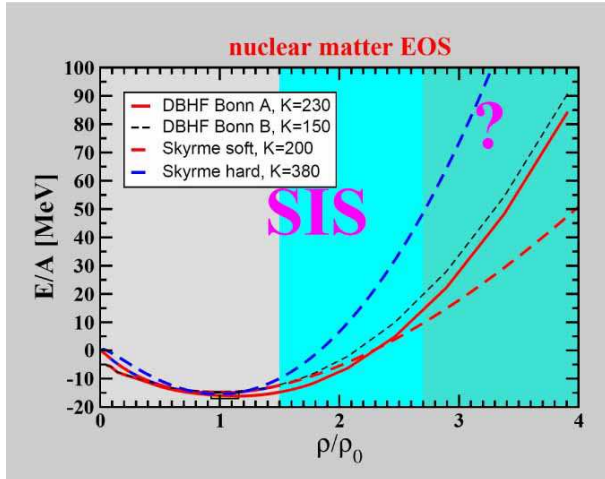


FIG. 2: Nuclear matter equations-of-state obtained from relativistic Dirac-Brueckner Hartree-Fock calculations and from a phenomenological model based on Skyrme forces. Both approaches assume different values for the compressibility (see [2]).

The study of the equation-of-state (EOS) of symmetric nuclear matter is one of the most challenging goals of the nuclear collision experiments at GSI. The experimental observables related to the EOS are the collective flow of nucleons and the production of strange particles. Microscopic transport calculations indicate that the yield of kaons created in collisions between heavy nuclei at subthreshold beam energies ( $E_{beam} = 1.58$  GeV for  $NN \rightarrow K^+ \Lambda N$ ) is sensitive to the EOS of nuclear matter at high baryon densities [3, 4]. This sensitivity is due to the production mechanism of  $K^+$  mesons. At subthreshold beam energies, the production of kaons requires multiple nucleon-

nucleon collisions or secondary collisions such as  $\pi N \rightarrow K^+ \Lambda$ . These processes are expected to occur predominantly at high baryon densities, and the densities reached in the fireball depend on the nuclear equation-of-state [5]. According to transport calculations, in central Au+Au collisions the bulk of  $K^+$  mesons is produced at nuclear matter densities larger than twice saturation density.

Moreover,  $K^+$  mesons are well suited to probe the properties of the dense nuclear medium because of their long mean free path. The propagation of  $K^+$  mesons in nuclear matter is characterized by the absence of absorption (as they contain an antistrange quark) and hence kaons emerge as messengers from the dense phase of the collision. In contrast, the pions created in the high density phase of the collision are likely to be reabsorbed and most of them will leave the reaction zone in the late phase.

The influence of the medium on the  $K^+$  yield is amplified by the steep excitation function of kaon production near threshold energies. Early transport calculations find that the  $K^+$  yield from Au+Au collisions at subthreshold energies will be enhanced by a factor of about 2 if a soft rather than a hard equation-of-state is assumed [3, 4]. Recent calculations take into account the modification of the kaon properties in the dense nuclear medium [6, 7] (see next chapter). When assuming a repulsive  $K^+N$  potential as proposed by various theoretical models (see [8] and references therein) the energy needed to create a  $K^+$  meson in the nuclear medium is increased and hence the  $K^+$  yield will be reduced. Therefore, the yield of  $K^+$  mesons produced in heavy ion collisions is affected by both the nuclear compressibility and the in-medium kaon potential.

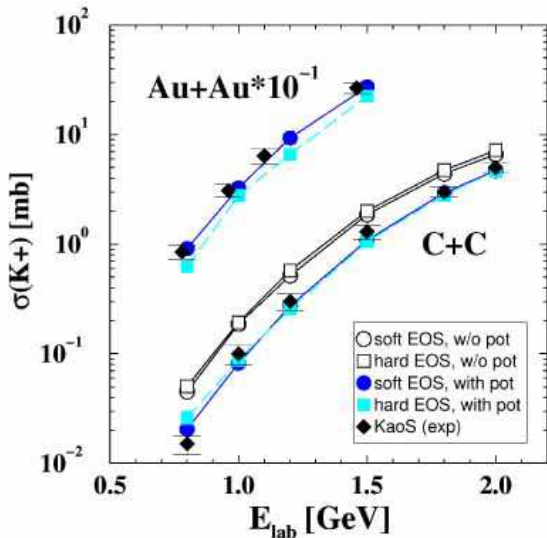


FIG. 3: Production cross sections of  $K^+$  mesons for Au+Au and C+C collisions as a function of the projectile energy per nucleon. The data (full diamonds) are compared to results of transport calculations assuming a soft (circles) and a hard (squares) nuclear equation-of-state with and without  $K^+N$  in-medium potentials. Taken from [2].

The KaoS collaboration proposed to disentangle these two competing effects by studying  $K^+$  production in a very light ( $^{12}\text{C}+^{12}\text{C}$ ) and a heavy collision system ( $^{197}\text{Au}+^{197}\text{Au}$ ) at different beam

energies near threshold [9]. The reaction volume is more than 15 times larger in Au+Au than in C+C collisions and hence the average baryonic density - achieved by the pile-up of nucleons - is significantly higher [7]. Moreover, the maximum baryonic density reached in Au+Au collisions depends on the nuclear compressibility [4, 10] whereas in the small C+C system this dependence is very weak [11].

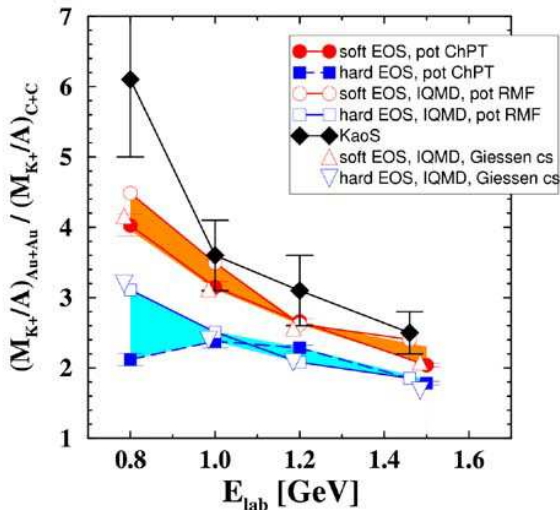


FIG. 4:  $K^+$  ratio measured in inclusive Au+Au and C+C collisions as function of beam energy [9]. The data are compared to various QMD calculations assuming nuclear compressibilities of  $\kappa = 200$  MeV and 380 MeV . Figure taken from [2].

Recent QMD transport calculations which take into account a repulsive kaon-nucleon potential reproduce the energy dependence of the kaon ratio if a compression modulus of  $\kappa = 200$  MeV for nuclear matter is assumed [11]. These calculations use momentum-dependent Skyrme forces to determine the compressional energy per nucleon (i.e. the energy stored in compression) as function of nuclear density (see figure 2). The result of this calculation is presented in figure 3 in comparison with the data [9].

In order to reduce systematic uncertainties both in experiment (normalization, efficiencies, acceptances etc.) and theory (elementary cross sections etc.) the  $K^+$  multiplicities are plotted as ratios  $(K^+/A)_{Au+Au} / (K^+/A)_{C+C}$  in figure 4. In this representation also the in-medium effects cancel to a large extent. The calculations are performed with a compression modulus of  $\kappa = 380$  MeV (a "hard" equation-of-state) and with  $\kappa = 200$  MeV (a "soft" equation-of-state) [2, 11]. The data clearly favor a soft equation of state (see figure 4).

## B. In-medium properties of kaons and antikaons

According to various calculations, the properties of kaons and antikaons are modified in dense baryonic matter (see e.g. [7, 8, 12]). In mean-field calculations, this effect is caused by a repulsive

$K^+N$  potential and an attractive  $K^-N$  potential. As a consequence, the total energy of a kaon at rest in nuclear matter increases and the antikaon energy decreases with increasing density. It has been speculated that an attractive  $K^-N$  potential will lead to Bose condensation of  $K^-$  mesons in the core of neutron stars above baryon densities of about 3 times saturation density [13].

A comparison of experimental data to results of various transport model calculations is presented in figure 5. The figure shows the  $K^+$  multiplicity densities  $dN/dy$  for near-central Ni+Ni collisions at 1.93 AGeV as function of the c.m. rapidity. Figure 5 combines data measured by the KaoS Collaboration [14] and by the FOPI Collaboration [15, 16]. The transport calculations clearly disagree with the data if in-medium effects are neglected (open symbols). However, when taking into account a repulsive  $K^+N$  potential, the  $K^+$  yield is reduced, and the calculations agree with the data sufficiently well (full symbols).

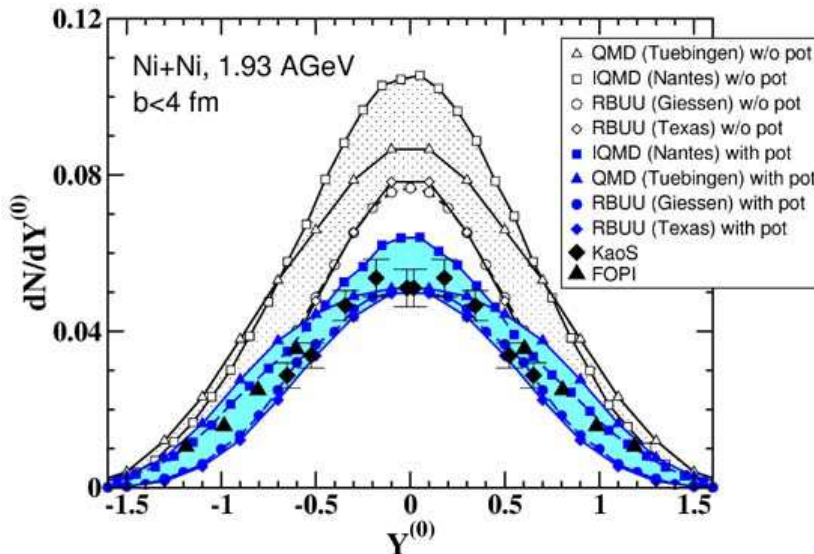


FIG. 5: Multiplicity density distributions of  $K^+$  mesons for near-central ( $b < 4.4$  fm) Ni+Ni collisions at 1.93 AGeV. Full black diamonds: KaoS data [14], full black triangles: FOPI data [15, 16]. The data are compared to various transport calculations. Full symbols: with in-medium effects. Open symbols: without in-medium effects. Taken from [2]

Another observable consequence of in-medium  $KN$  potentials is their influence on the propagation of kaons and antikaons in heavy-ion collisions. The measured azimuthal emission patterns of  $K^+$  mesons contradict the expectations based on a long mean free path in nuclear matter. The particular feature of sideward flow [17] and the pronounced out-of-plane emission around midrapidity [18] indicate that  $K^+$  mesons are repelled from the regions of increased baryonic density as expected for a repulsive  $K^+N$  potential [19, 20].

Figure 6 depicts the azimuthal angle distributions of  $K^+$  mesons measured in Au+Au collisions at 1.0 AGeV (left panel) and in Ni+Ni collisions at a beam energy of 1.93 AGeV (right panel). The  $K^+$  emission patterns clearly are peaked at  $\phi=\pm 90^\circ$  which is perpendicular to the reaction plane. Such a behavior is known from pions which are shadowed by the spectator fragments. In the case of  $K^+$  mesons, however, the anisotropy can be explained by transport calculations only if a repulsive in-medium  $K^+N$  potential is assumed. A flat distribution is expected when neglecting the in-medium potential [2, 21].

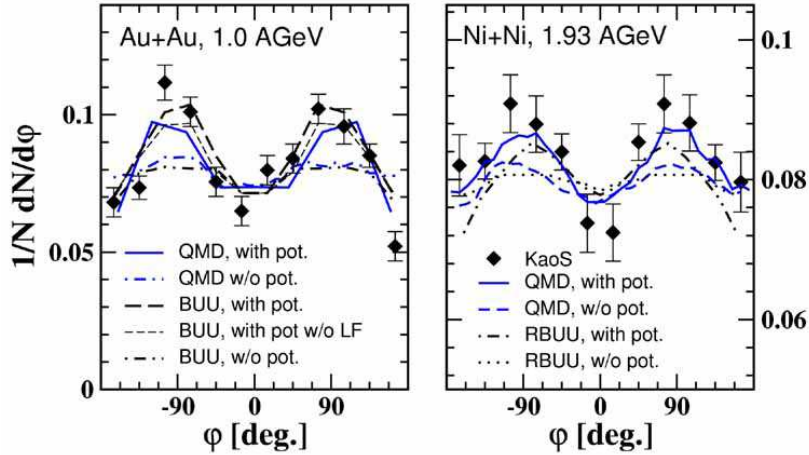


FIG. 6:  $K^+$  azimuthal distributions for semi-central Au+Au at 1 AGeV (left panel) and for Ni+Ni collisions at 1.93 AGeV (right panel). The data (full symbols) are compared to various transport calculations with and without in-medium potentials (see insert). Taken from [2], see also [21].

The key observable for the  $K^-N$  in-medium potential is the azimuthal emission pattern of  $K^-$  mesons. The existence of an attractive  $K^-N$  potential will strongly reduce the absorption of  $K^-$  mesons, and consequently the  $K^-$  mesons will be emitted almost isotropically in semicentral Au+Au collisions [20]. This observation would be in contrast to the behavior of pions and  $K^+$  mesons, and would provide strong experimental evidence for in-medium modifications of antikaons. Figure 7 depicts the first data on the  $K^-$  azimuthal emission pattern measured in heavy-ion collisions (lower panel) which differs significantly from the corresponding  $K^+$  and pion pattern (center and upper panel) [22]. First IQMD calculations with and without in-medium potentials for  $K^+$  and  $K^-$  mesons are able to reproduce the data [23]. Further clarification will come from high statistics data which have been measured in Au+Au collisions at 1.5 AGeV, and which are presently being analyzed.

In the mean field calculations as discussed above the  $K^-$  mesons are treated as quasi-particles

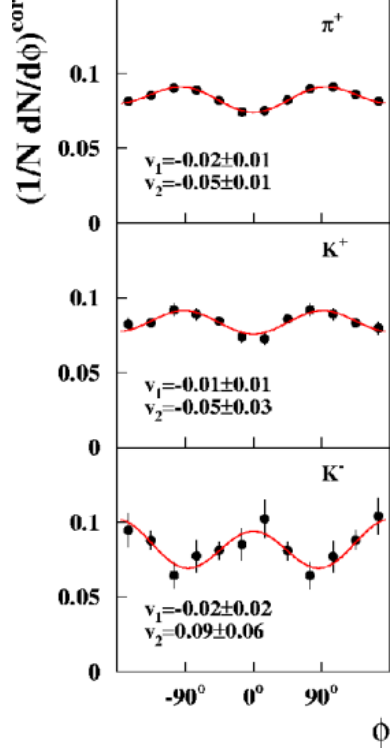


FIG. 7:  $\pi^+$ ,  $K^+$  and  $K^-$  azimuthal distribution for semi-central Ni+Ni collisions at 1.93 AGeV [22]. The data are corrected for the resolution of the reaction plane and refer to impact parameters of  $3.8 \text{ fm} < b < 6.5 \text{ fm}$ , rapidities of  $0.3 < y/y_{\text{beam}} < 0.7$  and momenta of  $0.2 \text{ GeV}/c < p_t < 0.8 \text{ GeV}/c$ . The lines represent Fourier expansions fitted to the data. The resulting coefficients are indicated.

which are on the mass shell. Microscopic coupled-channel calculations based on a chiral Lagrangian, however, predict a dynamical broadening of the  $K^-$  meson spectral function in dense nuclear matter [24, 25]. First off-shell transport calculations using  $K^-$  meson spectral functions have been performed [26]. The ultimate goal of the calculations is to relate the in-medium spectral function of  $K^-$  mesons to the anticipated chiral symmetry restoration at high baryon density. New experimental information on the in-medium modification of vector mesons is expected from the dilepton experiments with HADES at GSI. Highest baryon densities will be produced and explored with the Compressed Baryonic Matter (CBM) experiment at the future FAIR accelerator center in Darmstadt.

## II. TOWARDS HIGHEST BARYON DENSITIES

The future international Facility for Antiproton and Ion Research (FAIR) in Darmstadt will provide unique research opportunities in the fields of nuclear, hadron, atomic and plasma physics [27]. The accelerators will deliver primary beams (protons up to 90 GeV, Uranium up to 35 AGeV, nuclei with  $Z/A = 0.5$  up to 45 AGeV) and secondary beams (rare isotopes and antiprotons) with high intensity and quality. The aim of the nucleus-nucleus collision research program is to explore the QCD phase diagram at high net baryon densities and moderate temperatures. This approach



is complementary to the studies of matter at high temperatures and low net baryon densities performed at RHIC and LHC. At high baryon densities, new phases of strongly interacting matter are expected [1, 28, 29]. This exciting new field of high baryon density QCD needs input from experimental data, which can only be provided by new and dedicated nucleus-nucleus collision experiments.

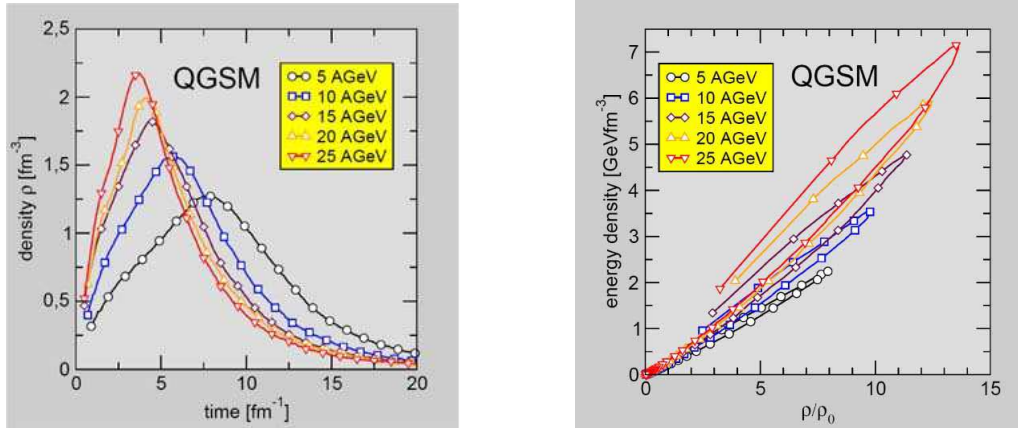


FIG. 8: Left panel: nuclear density in the inner volume of central Au+Au collisions as function of time calculated with the Quark Gluon String Model QGSM for beam energies between 5 and 25 AGeV [30]. Right panel: Corresponding energy density as function of the baryon density (in units of saturation density).

Very high baryon densities - which are comparable to those in the core of neutron stars - are predicted to be reached in heavy-ion collisions already at moderate beam energies. This is illustrated in figure 8 (left panel) which depicts the density in the inner volume of central Au+Au collisions as function of time calculated with a transport code (quark gluon string model QGSM, see [30]). Already at a beam energy of 5 AGeV the baryon density exceeds a value of  $1 \text{ fm}^{-3}$ , i.e. more than 6 times saturation density. The corresponding energy density is plotted in the right panel of figure 8 as function of baryon density (in units of saturation density). At a beam energy of 5 AGeV the energy density is predicted to reach a value of  $2 \text{ GeV fm}^{-3}$  which is - according to lattice QCD calculations - already beyond the deconfinement phase transition.

Trajectories of nucleus-nucleus collisions in the  $T - \mu_B$  plane have been calculated with a 3-fluid hydrodynamics model [31]. Figure 9 depicts the trajectories corresponding to different beam energies. The phase diagram also contains the critical endpoint (star) which has been predicted recently by lattice QCD calculations [32, 33]. The lattice calculations find a first order phase transition above  $\mu_B \approx 400 \text{ MeV}$ , and a smooth cross over from hadronic to partonic matter below this value. The hydrodynamics model calculation indicates that this critical endpoint might be found in the vicinity of the freeze-out point of a central Pb+Pb collision at a beam energy of about

30 AGeV.

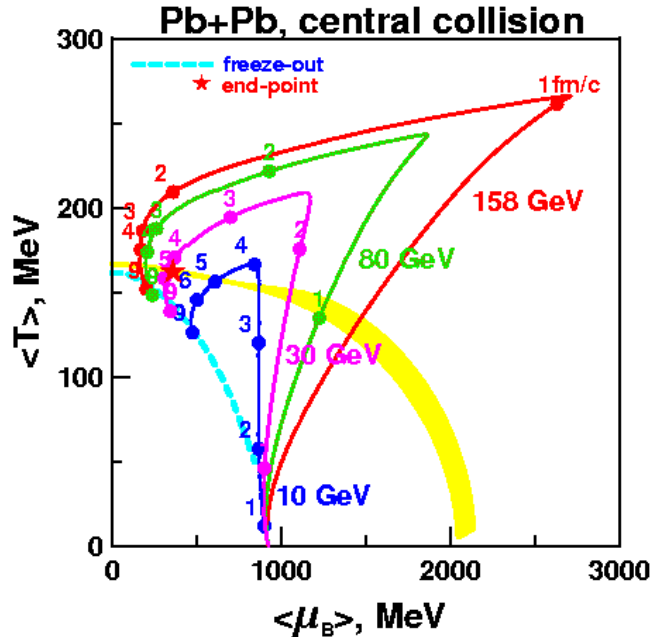


FIG. 9: Trajectories of heavy ion collisions in the QCD phase diagram calculated by a 3-fluid hydrodynamics model [31]. Dashed line: chemical freeze-out curve. Star: critical endpoint.

The CERN-NA49 collaboration found a pronounced peak in the excitation function of the  $K^+/\pi^+$  ratio in central Pb+Pb collisions at a beam energy of 30 AGeV [34]. This structure cannot be explained by any theoretical model. The Lambda/pion ratio exhibits also a maximum at the same beam energy. In this case, the shape of the excitation function can be reproduced by a statistical model analysis, which indicates that the transition from baryon dominated matter to meson dominated matter occurs at a beam energy of about 30 AGeV. It turns out that the maximum net-baryon density at freeze-out is reached at a beam energy of 30 AGeV [35].

### A. Experimental observables

The major challenge is to find diagnostic probes which are connected to the onset of chiral symmetry restoration, to the deconfinement phase transition, and to the equation of state of hadronic and partonic matter.

The in-medium spectral functions of short-lived vector mesons - which are expected to be sensitive to chiral symmetry restoration - can be studied in the dense nuclear medium via their decay into lepton pairs [36]. Since the leptons are very little affected by the passage through the

high-density matter, they provide, as a penetrating probe, almost undistorted information on the conditions in the interior of the collision zone. Another observable sensitive to in-medium effects is open charm, e.g. D-mesons. The effective masses of D-mesons - a bound state of a heavy charm quark and a light quark - are expected to be modified in dense matter similarly to those of kaons. Such a change would be reflected in the relative abundance of charmonium ( $c\bar{c}$ ) and D-mesons.

The onset of a first order phase transition is expected to cause a discontinuity in the excitation function of particular observables. Such a non-monotonic behavior has been observed around 30 AGeV in the kaon-to-pion ratio and in the inverse slope parameter of kaons [34]. A beam energy scan looking at a variety of observables is needed to clarify the experimental situation. This includes the measurement of the phase-space distributions of strange particles, in particular multi-strange baryons (anti-baryons), and particles containing charm quarks. For example, a discontinuity in the excitation function of the  $J/\psi$ -to- $\psi'$  ratio would indicate sequential charmonium dissociation due to color screening in the deconfined phase. Moreover, event-by-event fluctuations are expected to appear when crossing a first order phase transition, and particularly in the vicinity of the critical endpoint. The identification of a critical point would provide direct evidence for the existence and the character of a deconfinement phase transition in strongly interacting matter.

The formation of a mixed phase indicating the onset of deconfinement leads to a softening of the equation of state at a given beam energy [37]. The location of the so called softest point (i.e. where the sound velocity exhibits a minimum) may be discovered by measuring carefully the excitation function of the collective flow of particles.

Charm production plays a particular role at FAIR energies, because charmonium, D-mesons and charmed hyperons are created at beam energies close to the kinematical threshold. Therefore, these particles are sensitive probes of the early, high-density stage of the collision (more than 10 times saturation density !). Collective effects contributing to charm production may be visible for the first time. Charm exchange processes may become important, revealing basic properties of charm propagation in a dense baryonic medium. The situation is analogue to strangeness production at SIS18 energies, where 2-3 times saturation density is probed in Au+Au collisions. In order to perform high statistics measurements, the low cross sections for charm production at threshold beam energies has to be compensated by high beam intensities.

## B. The CBM detector

The experimental task is to identify both hadrons and leptons and to detect rare probes in a heavy ion environment. The apparatus has to measure multiplicities and phase-space distributions of hyperons, light vector mesons, charmonium and open charm (including the identification of protons, pions and kaons) with a large acceptance. The challenge is to filter out those rare probes in Au+Au (or U+U) collisions at reaction rates of up to  $10^7$  events per second. The charged particle multiplicity is about 1000 per central event. Therefore, the experiment has to fulfill the following requirements: fast and radiation hard detectors, large acceptance, lepton and hadron identification, high-resolution secondary vertex determination and a high speed trigger and data acquisition system. The layout of the CBM experimental setup is sketched in figure 10.

The CBM setup consists of a the following subsystems:

- a large acceptance superconducting dipole magnet
- a radiation-hard Silicon Tracking Station comprizing pixel/strip detectors
- a Silicon pixel microvertex detector with high position resolution and low material budget
- a Ring Imaging Cherenkov detector (RICH) for soft electron identification
- Transition Radiation Detectors (TRD) for identification of electrons with momenta above 2 GeV/c
- a muon detection system consisting of several layers of absorbers and tracking chambers. This system is an alternative to RICH and TRDs, which then would be used as tracking stations for hadron identification.
- Resistive Plate Chambers (RPC) for time of flight measurement (hadron identification)
- an Electromagnetic calorimeter (ECAL) for identification of photons
- a high speed online event selection and data acquisition system

The CBM detector is designed for a comprehensive research program using proton beams (with energies of 10 - 90 GeV) and nuclear beams (10 - 45 AGeV) impinging on various targets. The measurements at beam energies below 10 AGeV will be performed with the HADES detector. The measurements, in particular those of rare diagnostic probes, require a dedicated accelerator with

high beam intensities, large duty cycle, excellent beam quality, and with an operational availability of several month per year. Details of the CBM research program and of the setup can be found in the Technical Status report which has been submitted in January 2005 [38]. The CBM Collaboration actually consists of about 350 persons from 41 institutions and 15 countries.

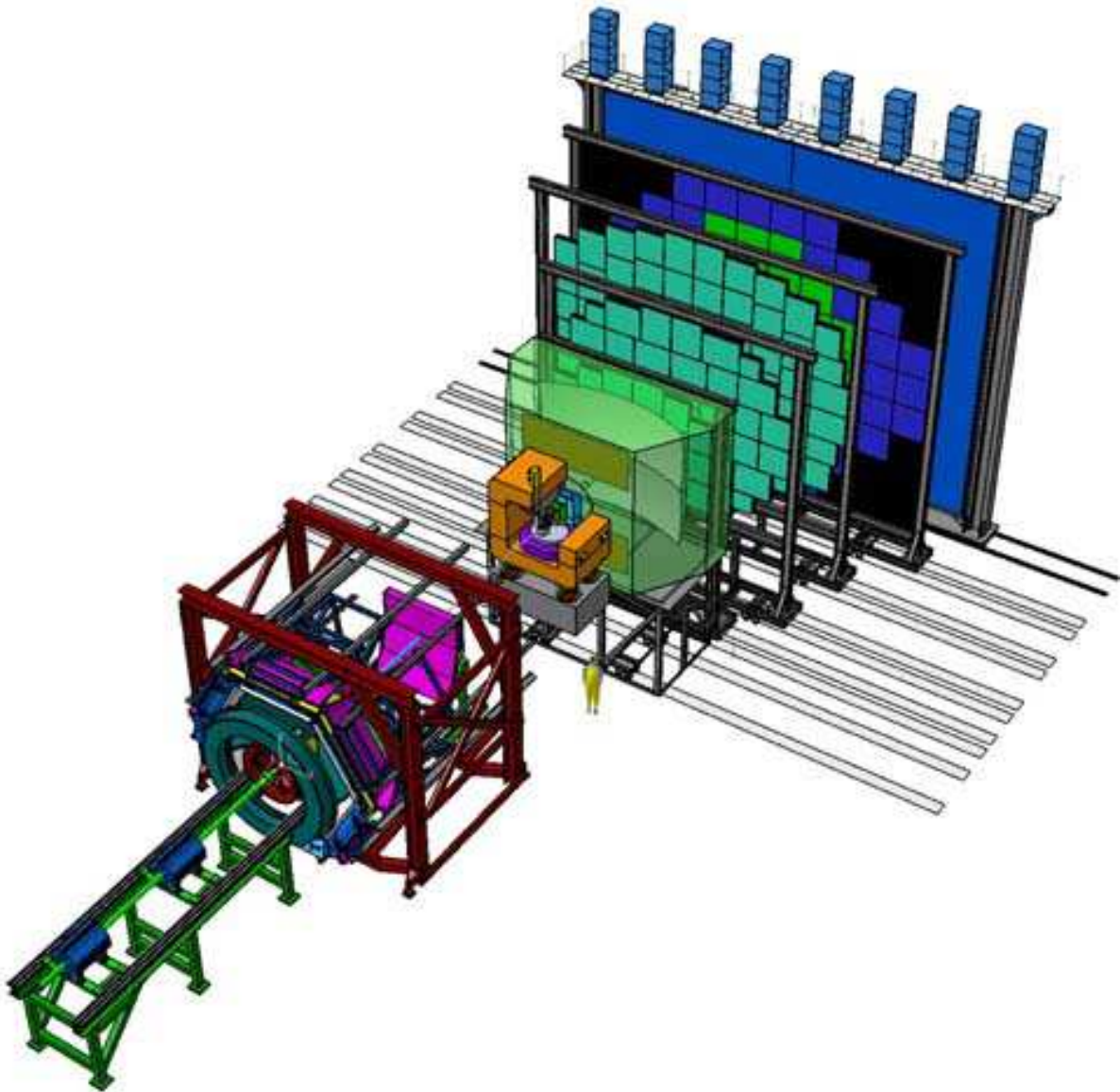


FIG. 10: Sketch of the planned Compressed Baryonic Matter (CBM) experiment together with the HADES detector.

## Acknowledgements

I would like to thank my colleagues of the KaoS collaboration who have measured most of the data on strangeness production at SIS presented in this paper: I. Böttcher, M. Dębowski, F. Dohrmann, A. Förster, E. Grosse, P. Koczoń, B. Kohlmeier, F. Laue, M. Menzel, L. Naumann, H. Oeschler, M. Ploskon, W. Scheinast, E. Schwab, Y. Shin, H. Ströbele, C. Sturm, G. Surówka, F. Uhlig, A. Wagner, W. Waluś.

The CBM project is supported by EU under RII3-CT-2004-506078 HADRONPHYSICS and by INTAS Ref. Nr. 03-51-6645.

- 
- [1] F. Weber, *J. Phys. G*, *Nucl. Part. Phys.* **27** (2001) 465
  - [2] C. Fuchs, *Prog.Part.Nucl.Phys.* 56 (2006) 1
  - [3] J. Aichelin, C. M. Ko, *Phys. Rev. Lett.* **55** (1985) 2661
  - [4] G. Q. Li, C. M. Ko, *Phys. Lett.* **B 349** (1995) 405
  - [5] C. Fuchs et al., *Phys. Rev.* **C 56** (1997) R606
  - [6] C.M. Ko and G.Q. Li, *J. Phys.* **G 22** (1996) 1673
  - [7] W. Cassing and E. Bratkovskaya, *Phys. Rep.* **308** (1999) 65
  - [8] J. Schaffner-Bielich, J. Bondorf, I. Mishustin, *Nucl. Phys.* **A 625** (1997) 325
  - [9] C. Sturm et al., *Phys. Rev. Lett.* **86** (2001) 39
  - [10] J. Aichelin, *Phys. Rep.* **202** (1991) 233
  - [11] C. Fuchs et al., *Phys. Rev. Lett.* **86** (2001) 1974
  - [12] G.E. Brown et al., *Phys. Rev.* **C 43** (1991) 1881
  - [13] G.Q. Li, C.H. Lee and G.E. Brown, *Phys. Rev. Lett.* **79** (1997) 5214
  - [14] M. Menzel et al., *Phys. Lett.* **B 495** (2000) 26
  - [15] D. Best et al., *Nucl. Phys.* **A 625** (1997) 307
  - [16] K. Wisniewski et al., *Eur. Phys. J.* **A 9** (2000) 515
  - [17] P. Crochet et al., *Phys. Lett.* **B 486** (2000) 6
  - [18] Y. Shin et al., *Phys. Rev. Lett.* **81** (1998) 1576
  - [19] G.Q. Li, C.M. Ko, G.E. Brown, *Phys. Lett.* **B 381** (1996) 17
  - [20] Z.S. Wang et al., *Eur. Phys. J.* **A 5** (1999) 275
  - [21] A. Larionov and U. Mosel, *Phys. Rev. C* 72 (2005) 014901
  - [22] F. Uhlig et al., *Phys. Rev. Lett.* **95** (2005) 012301
  - [23] C. Hartnack et al., *Eur. Phys. J.* **A 1** (1998) 151
  - [24] T. Waas, N. Kaiser and W. Weise, *Phys. Lett.* **B 379** (1996) 34
  - [25] M. F. M. Lutz and C. Korpa, *Nucl. Phys.* **A 700**(2002) 209

- [26] W. Cassing et al., Nucl.Phys. **A 727** (2003) 59
- [27] An International Accelerator Facility for Beams of Ions and Antiprotons, Conceptional Design Report 2001,  
<http://www.gsi.de/GSI-Future/cdr/>
- [28] F. Wilczek, Physics Today **53** (2000) 22
- [29] M. Stephanov, K. Rajagopal, E. Shuryak, Phy. Rev. **D 60** (1999) 114028
- [30] G. Baur et al., Phys.Rev. **C71** (2005) 054905
- [31] Y. Ivanov, V. Russkikh, V.Toneev, Phys.Rev. **C73** (2006) 044904
- [32] Z. Fodor and S.D. Katz, JHEP **0404** (2004) 050
- [33] S. Ejiri et al., hep-lat/0312006, Prog.Theor.Phys.Suppl. 153 (2004) 118
- [34] C. Blume et al., J. Phys. **G 31** (2005) 685
- [35] J. Cleymans et al., Phys. Rev. **C 73** (2006) 034905
- [36] R. Rapp and J. Wambach, Nucl. Phys. **A 661** (1999) 33c
- [37] C. M. Hung and E. V. Shuryak, Phys. Rev. Lett. **75** (1995) 4003
- [38] CBM Technical Status Report 2005  
[http://www-linux.gsi.de/~hoehne/report/cbmtsr\\_public.pdf](http://www-linux.gsi.de/~hoehne/report/cbmtsr_public.pdf)